Natural Products and Bioprospecting

ORIGINAL ARTICLE

Open Access

New seco-anthraquinone glucoside from the roots of *Rumex crispus*

Yong-Xiang Li[1,2], Na Li[1], Jing-Juan Li[1], Man Zhang[1], Hong-Tao Zhu[1], Dong Wang[1] and Ying-Jun Zhang[1,3*]

Abstract

A new seco-anthraquinone, crispuside A (**1**), and three new 3,4-dihydronaphthalen-1(2*H*)-ones, napthalenones A-C (**2**–**4**), were isolated from the roots of *Rumex crispus* L., along with 10 known anthraquinones (**6–14**) and naphthalenone (**5**). Their structures were fully determined by extensive spectroscopic analyses, including ECD, and X-ray crystallography in case of compound **5**, whose absolute configuration was determined for the first time. The isolates **1**, **6**–**14** were evaluated for their anti-inflammatory and anti-fungal activity against three skin fungi, e.g., *Epidermophyton floccosum*, *Trichophyton rubrum*, and *Microsporum gypseum*. Most of the isolates showed weak anti-fungal and anti-inflammatory activity. Only compound **9** exhibited obvious anti-fungal activity against *E. floccosum* ($MIC_{50} = 2.467 \pm 0.03$ μM) and *M. gypseum* ($MIC_{50} = 4.673 \pm 0.077$ μM), while the MIC_{50} values of the positive control terbinafine were 1.287 ± 0.012 and 0.077 ± 0.00258 μM, respectively. The results indicated that simple emodin type anthraquinone is more potential against skin fungi than its oxyglucosyl, *C*-glucosyl and glycosylated seco analogues.

Keywords: Polygonaceae, *Rumex crispus* L., Anthranoids, Anti-fungal activity

*Correspondence: zhangyj@mail.kib.ac.cn

[1] State Key Laboratory of Phytochemistry and Plant Resources in West China, Kunming Institute of Botany, Chinese Academy of Sciences, Kunming 650204, People's Republic of China
Full list of author information is available at the end of the article

Graphical Abstract

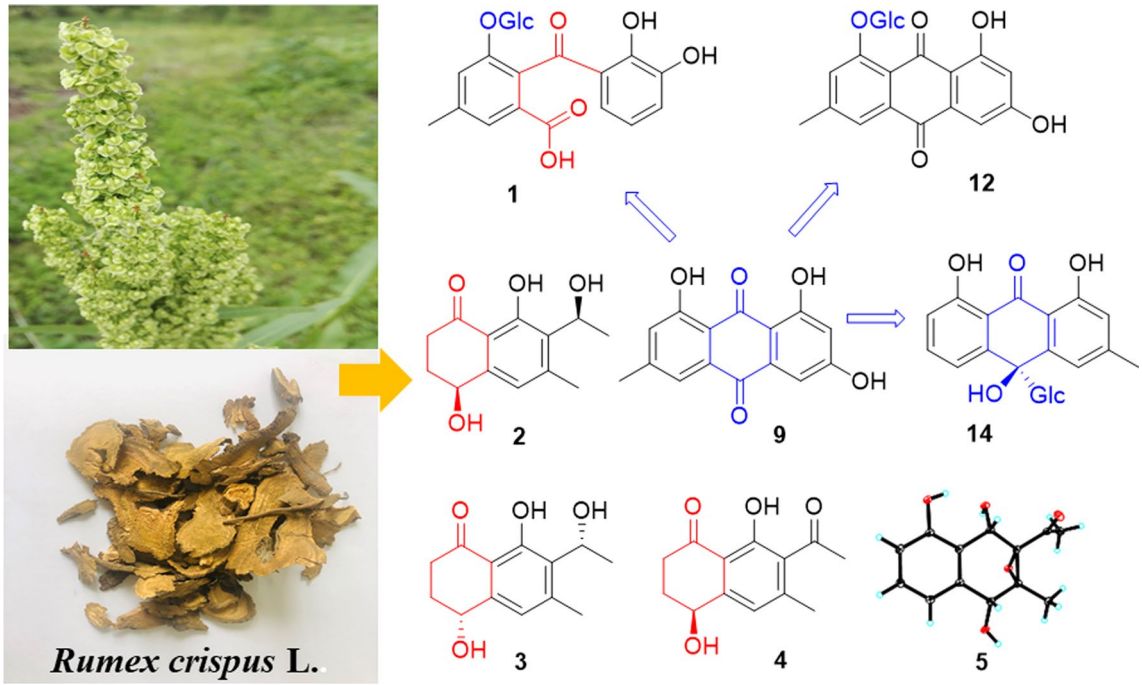

1 Introduction

The genus *Rumex* with more than 200 species distributing widely in the world is the second largest genus in the family Polygonaceae, in which some species displayed nutritional and medicinal properties. For example, *Rumex patientia* L. was reported having abundant amino acid and cellulose [1]. A series of anthranoids, tannins, naphthalenes, and flavonoids were identified as the major chemical compositions from *Rumex* species [2–5].

Rumex crispus L., a perennial herbaceous species with stout and straight root system, is widely distributed in China, Korea, Kazakhstan, Russia, Japan, Europe, and North America [6, 7]. It has been used medicinally for treating jaundice and related liver diseases, stomachache, neckache, low blood pressure, pneumonia, wound healing, and rheumatism [8–10]. The crude extract was reported to possess anti-inflammatory, antimicrobial, antioxidant, and anti-diabetic properties [11–14]. However, the chemical compositions are so far not well-known. Our detailed phytochemical study on the roots of *R. crispus* led to the isolation of four new compounds including a seco-anthraquinone glucoside (**1**) and three naphtholones (**2–4**), along with 10 known anthraquinones (**6–14**) and napthalenone (**5**) (Fig. 1). Most of the isolates, **1** and **6–14**, were evaluated for their anti-fungal activity against three skin fungi (*Epidermophyton floccosum*, *Trichophyton rubrum*, *Microsporum gypseum*), and the anti-inflammatory properties. Herein, we report the study.

2 Result and discussion

The air-dried roots of *R. crispus* were crushed into small grains and extracted with 90% aqueous MeOH. After removal of the organic solvent, the crude extract was suspended into water and fractionated with ethyl acetate. The ethyl acetate fraction was further applied to repeated column chromatography (CC) over Sephadex LH-20, macroporous resin D101, silica gel, and RP-18, followed with semipreparative HPLC, yielded 14 compounds. Among which, one seco-anthraquinone glucoside (**1**) and three naphtholones (**2–4**) are new compounds. Ten known compounds were identified as 3-acetyl-2-methyl-1,4,5-trihydroxy-2,3-epoxynaphthoquinol (**5**) [15], nepalensides A (**6**) and B (**7**) [16], polyanthraquinoside A (**8**) [17], emodin (**9**) [18], physcion (**10**) [19], chrysophanol (**11**) [20], emodin-1-*O*-*β*-D-glucopyranoside (**12**) [21], 6-methoxyl-10-hydroxyaloin B (**13**) [22], (10*R*)-3-methyl-1,8,10-trihydroxy-10-D-glucopyranosyl-9(10*H*)-anthracenone (**14**) [23] (Fig. 1), respectively, by comparison of their spectroscopic data

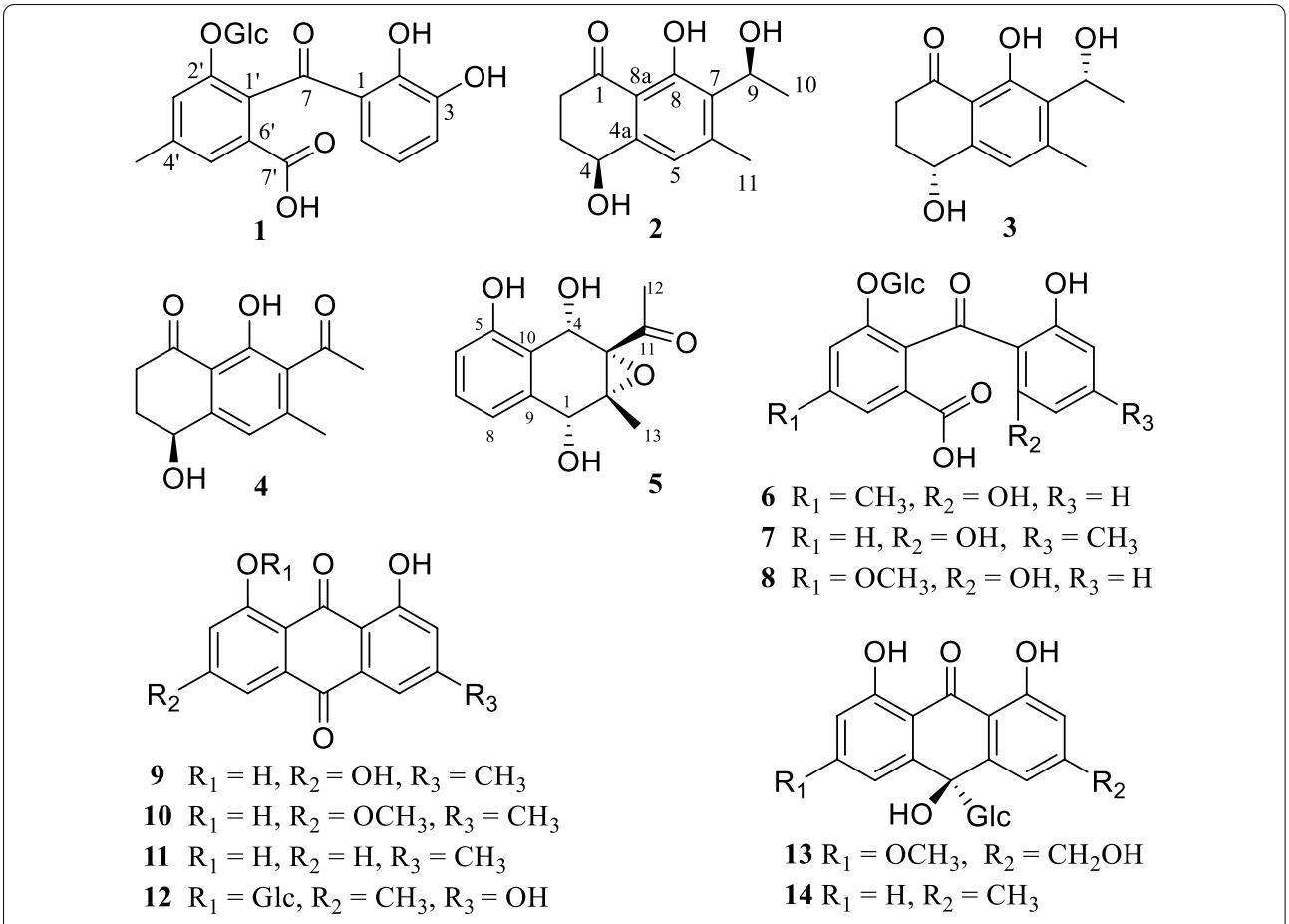

Fig. 1 Compounds **1**–**14** isolated from the roots of *Rumex crispus* L.

with literature values. Seven compounds, **5**–**8** and **12**–**14**, were isolated from *R. crispus* for the first time.

2.1 Structural identification of compounds

Compound **1** was obtained as yellowish amorphous powder. Its molecular formula, $C_{21}H_{22}O_{11}$, was determined by negative HRESI-TOF–MS (*m/z* 449.1094 $[M–H]^-$, calcd. for $C_{21}H_{21}O_{11}$, 449.1089). In the ^{13}C NMR spectrum of **1** (Table 1), 14 carbon signals due to one ketone (δ_C 203.3), one carboxyl (δ_C 170.8) and two benzene ring (δ_C 106.0–165.0, 12 × C) were observed, assignable to a carboxylated benzophenone. In addition, 6 carbon signals at δ_C 101.3 (C-1″), 74.7 (C-2″), 78.2 (C-3″), 71.7 (C-4″), 77.8 (C-5″), and 62.5 (C-6″) from a glucosyl moiety and a methyl signal at δ_C 21.4 were also observed. In the ^1H NMR spectrum of **1**, three characteristic proton resonances at δ_H 6.61 (1H, d, J = 8.3 Hz, H-4), 7.36 (1H, t, J = 8.3 Hz, H-5) and 6.56 (1H, d, J = 8.3 Hz, H-6) suggested the existence of a 1,2,3-trisubstituted benzene ring [24]. Moreover, two aromatic singlet resonances at δ_H 6.90 (1H, s, H-3′) and 7.34 (1H, br s, H-5′)] and a 3-H singlet signal at δ_H 2.38 (3H, s) due to a methyl group were observed, together with one anomeric proton at δ_H 4.85 (1H, d, J = 7.8, H-1″) and a set of proton signals in the range between δ_H 2.3–3.8, disclosing the existence of

Table 1 ^1H (600 MHz) and.^{13}C (150 MHz) NMR data of **1** in CD_3OD (δ in ppm, J in Hz)

No	δ_C, type	δ_H, mult. (J)	No	δ_C, type	δ_H, mult. (J)
1	114.9, s		5′	122.8, d	7.34 br s
2	165.0, s		6′	132.3, s	
3	160.0, s		7′	170.8, s	
4	112.4, d	6.61 d (8.3)	Me	21.4, q	2.38 s
5	137.1, d	7.36 t (8.3)	1″	101.3, d	4.85 d (7.8)
6	106.0, d	6.56 d (8.3)	2″	74.7, d	2.45 m
7	203.3, s		3″	78.2, d	3.29 m
1′	130.3, s		4″	71.1, d	3.27 m
2′	154.9, s		5″	77.8, d	3.14 t (9.4)
3′	121.8, d	6.90 s	6″	62.5, t	a 3.77 dd (12.1, 2.3)
4′	140.8, s				b 3.61 dd (12.1, 5.8)

a sugar moiety. The $J_{1''-2''}$ coupling constant of anomeric proton (7.8 Hz) revealed the glucosyl anomeric center to be β configuration. The ^{1}H and ^{13}C NMR data of **1** were closely related to those of **6** [16]. However, instead of a symmetric 1,2,3-trisubstituted benzene ring in **6**, an unsymmetric 1,2,3-trisubstituted benzene ring appeared in **1**. This was confirmed by the HMBC correlations of H-4 (δ_H 6.61) with C-1 (δ_C 114.9), C-2 (δ_C 165.0), C-3 (δ_C 160.0) and C-6 (δ_C 106.0), and H-6 (δ_H 6.56) with C-1 (δ_C 114.9), C-4 (δ_C 112.4) and C-7 (δ_C 203.3). Moreover, the HMBC correlations from methyl proton at δ_H 2.38 to C-3′ (δ_C 121.8), C-4′ (δ_C 140.8), and C-5′ (δ_C 122.8), from H-3′ (δ_H 6.90) to C-5′ and C-6′ (δ_C 132.3), and from H-5′ (δ_H 7.34) to C-3′, C-6′ and C-7′ (δ_C 170.8) (Fig. 2) confirmed the structure of **1**. Therefore, the structure of compound **1** was established as shown in Fig. 1 and named as crispuside A.

Compound **1** is a new anthraquinone-related compound, whose formation mechanism might be similar to that of desmethylsulochrin, which was established by the ring-opening process of questin catalyzed by GedF (Geodin synthesis protein F) and GedK [25]. In *R. crispus*, compound **1** maybe formed from reduction firstly and then ring-opening of ziganein-1-*O*-*β*-glucopyranoside catalyzed by GedF and GedK respectively (Fig. 3).

Compounds **2** and **3**, obtained as colorless powder, are a pair of enantiomers possessing the same molecular formula $C_{13}H_{16}O_4$, as deduced by the negative HRESIMS (*m/z* 235.0979 $[M-H]^-$ calcd $C_{13}H_{15}O_4$, 235.0976). The ^{1}H, ^{13}C NMR, and HSQC spectral data of **2** and **3** revealed the existence of two methyls [δ_H 2.48 (3H, s, H-11), δ_C 21.1; δ_H 1.52 (3H, d, J=6.7 Hz, H-10), δ_C 21.1], two methylenes [δ_H 2.88 (1H, m, H-2a), 2.67 (1H, m, H-2b), δ_C 35.9; δ_H 2.27 (1H, m, H-3a), 2.08 (1H, m, H-3b), δ_C 32.6], one aromatic methine [δ_H 6.89 (1H, s, H-5), δ_C 121.9], two oxymethines [δ_H (1H, 4.78, dd, J=8.0, 3.8 Hz, H-4), δ_C 68.1; δ_H 5.34 (1H, q, J=6.7 Hz, H-9), δ_C 65.6], one carbonyl group (δ_C 206.1, C-1), and a set of quaternary aromatic carbons (δ_C 146.4, 147.2, 130.9, 161.5, 114.6). These spectroscopic features were similar to those of (4*S*,9*S*)-9-hydroxy-*O*-methylasparvenone (4*S*,9*S*-HM) [26], whose molecular weight was 252 Da, 16 Da more than those of **2** and **3**. However, the chemical shifts of C-6 and C-11 in **2** and **3** were obviously different with those of 4*S*,9*S*-HM, indicating that the substituent at C-6 in **2** and **3** was methyl group, instead of a methoxyl group in 4*S*,9*S*-HM. Moreover, the HMBC correlations of H-11 (δ_H 2.48) with C-5 (δ_C 121.9), C-6 (δ_C 147.2) and C-7 (δ_C 130.9) confirmed the substitution of methyl at C-6 position. The ^{1}H–^{1}H COSY correlations between H-2 and H-3, and the key HMBC correlations from H-2

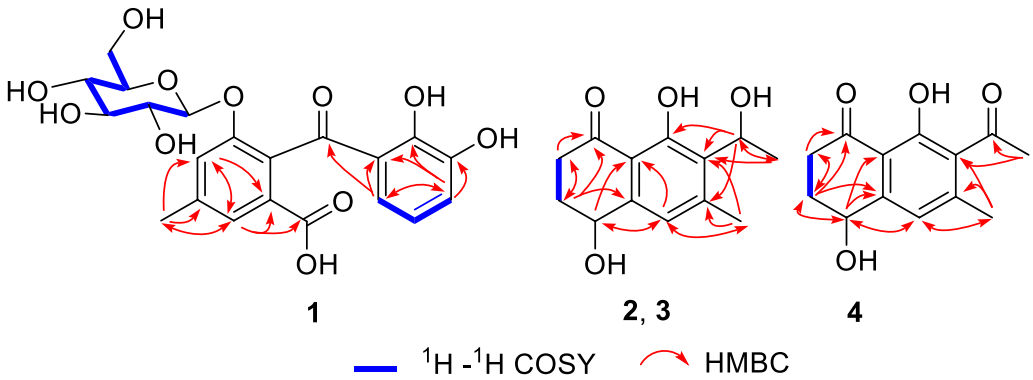

Fig. 2 Key ^{1}H–^{1}H COSY and HMBC correlations of **1**, **2**, **3** and **4**

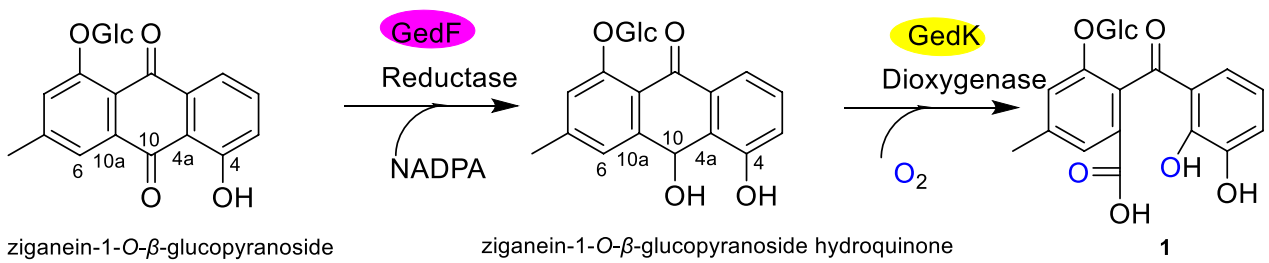

Fig. 3 Possible formation of compound **1**

to C-1/C-3, from H-3 to C-1/C-2, from H-4 to C-5/C-8a, from H-11 to C-5/C-6/C-7, from H-5 to C-8a, from H-10 to C-7/C-9, from H-9 to C-6/C-7/C-8 determined the planar structures of **2** and **3** as 4,8-dihydroxy-7-(1-hydroxyethyl)-6-methyl-3,4-dihydronaphthalen-1(2*H*)-one. Comparison of the experimental ECD spectrum of **2** with the calculated ECD (Fig. 4) of the four stereoisomers, (4*S*,9*S*)-, (4*R*,9*R*)-, (4*S*,9*R*)- and (4*R*,9*S*)- HM [26] showed the ECD of **2** was more comparable with the computationally derived data for (4*S*,9*S*)- and (4*S*,9*R*)- with positive Cotton effects (CEs) at 248 and 214 nm and negative CE at 280 nm. However, the CE amplitudes of **2** were notably closer to those of the (4*S*,9*S*)- diastereomer, thus favoring the (4*S*,9*S*) absolute configuration for **2**. Therefore, compound **2** was proposed as (4*S*,9*S*)-4,8-dihydroxy-7-(1-hydroxyethyl)-6-methyl-3,4-dihydronaphthalen-1(2*H*)-one. Similarly, the absolute configuration of **3** was deduced as (4*R*,9*R*)-4,8-dihydroxy-7-(1-hydroxyethyl)-6-methyl-3,4-dihydro-naphthalen-1(2*H*)-one. The structures of **2** and **3** were established as shown and named as naphthalenones A (**2**) and B (**3**), respectively.

Compound **4** was isolated as white powder. Its molecular formula was assigned to be $C_{13}H_{14}O_4$, as deduced from the HRESIMS (*m/z* 233.0814 $[M-H]^-$, calcd. $C_{13}H_{13}O_4$, 233.0814). The UV spectrum showed absorption bands at λ_{max} 286 nm. The 1D and 2D NMR data of **4** (Table 2) indicated it shared the same 3,4-dihydronaphthalen-1(2*H*)-one skeleton with **2**. The molecular weight of **4** is 2 Da less than that of **2**. Comparing the DEPT and ^{13}C NMR data of **4** with those of **2** indicated that, a ketone group (δ_C 206.5) appeared in **4**, instead of an oxymethine C-9 (δ_C 65.6) in **2**. This was further verified by the HMBC correlation of H-10 with C-9 in the HMBC spectrum of **4**. Comparing with the ECD curve of the known 7-acetyl-4*R*,8-dihydroxy-6-methyl-1-tetralone (ADMT) [27], compound **4** showed a negative CE at 260–270 nm in ECD spectrum, which is in contrast to ADMT (Fig. 4). Therefore, the structure of **4** was determined to be 7-acetyl-4*S*,8-dihydroxy-6-methyl-1-tetralone and named as naphthalenone C.

Compound **5** was isolated as colorless needle crystal with a molecular formula of $C_{13}H_{14}O_5$, as determined by the ESI–MS (negative ion mode) *m/z* 249 $[M-H]^-$, and ^{13}C NMR and DEPT spectroscopic data. The ^{13}C NMR spectrum of **5** showed one carbonyl (δ_C 208.6), six aromatic carbon signals (δ_C 157.4, 116.0, 129.9, 119.1, 137.8, 120.2) with three methines and one oxygenated quarternary carbon, and six sp^3 carbon signals (δ_C 70.2, 65.6, 72.6, 68.1, 29.1, 15.9) assignable to two methyls, two oxymethines and two oxy quarternary carbons. The ^1H NMR spectrum showed three characteristic proton resonances at δ_H 6.72 (1H, d, $J=7.9$ Hz, H-6), 7.17 (1H, t, $J=7.9$ Hz, H-7), 7.10 (1H, d, $J=7.9$ Hz, H-8) suggesting the existence of a 5,9,10-trisubstituted benzene ring. In addition, two methyls (δ_H 2.36, s, H-12; 1.47, s, CH_3-2) and two oxymethines (6.72, d, $J=7.9$ Hz, H-6; 5.57, s, H-4) signals were observed. The above data indicated that **5** was a naphthoquinol derivative, whose epoxide ring was inferred by chemical shifts (δ_C 65.6, C-2; δ_C 72.6, C-3) and seven degrees of unsaturation. The detailed analyses of the 2D NMR (^1H-^1H COSY, HMQC, HMBC) spectra (Fig. 5) deduced the planar structure of **5**, which is the same as the reported 3-acetyl-2-methyl-1,4,5-trihydroxy-2,3-epoxynaphthoquinol without determination of the absolute configuration [15]. In the present study,

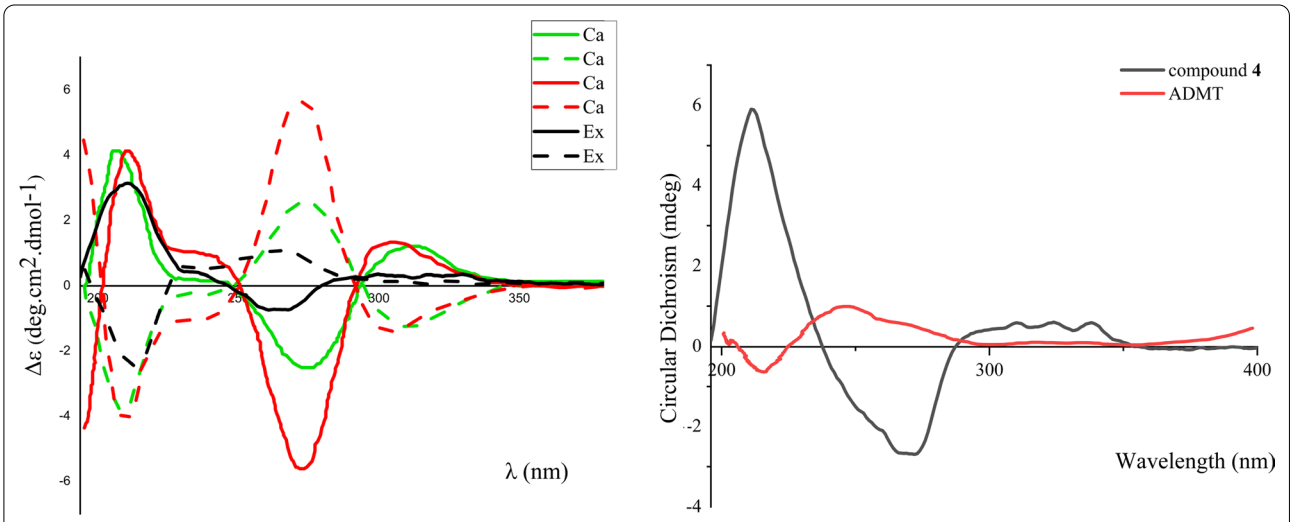

Fig. 4 Experimental ECD curves of **2**, **3**, **4** and ADMT, and calculated ECD curves of four stereoisomers of HM

Table 2 ^{1}H (600 MHz) and ^{13}C (150 MHz) NMR data of **2**, **3, 4** and **5** in CD_3OD (δ in ppm, *J* in Hz)

No	2, 3		4[a]		5[a]	
	δ_C, type	δ_H mult. (*J*)	δ_C, type	δ_H mult. (*J*)	δ_C, type	δ_H mult. (*J*)
1	206.1, s		205.6, s		70.2, d	4.62 s
2	35.9, t	a 2.88 m b 2.67 m	35.9, t	a 2.82 m b 2.64 m	65.6, s	
3	32.6, t	a 2.27 m b 2.08 m	32.4, t	a 2.25 overlap b 2.03 m	72.6, s	
4	68.1, d	4.78 dd (8.0, 3.8)	67.8, d	4.67 dd (8.7, 3.9)	68.1, d	5.57 s
4a	146.4, s		149.6, s			
5	121.9, d	6.89 s	120.9, d	6.89 s	157.4, s	
6	147.2, s		146.2, s		116.0, d	6.72 d (7.9 Hz)
7	130.9, s		130.4, s		129.9, d	7.17 t (7.9 Hz)
8	161.5, s		160.7, s		119.1, d	7.10 d (7.9 Hz)
8a	114.6, s		114.9, s			
9	65.6, d	5.34 q (6.7)	205.6, d		137.8, s	
10	22.0, q	1.52 d (6.7)	32.2, q	2.49 s	120.2, s	
11	21.1, q	2.48 s	20.5, q	2.25 s	208.6, s	
12					29.1, q	2.36 s
13					15.9, q	1.47 s

[a] Measured at 500 MHz for ^{1}H and 125 MHz for ^{13}C NMR, respectively

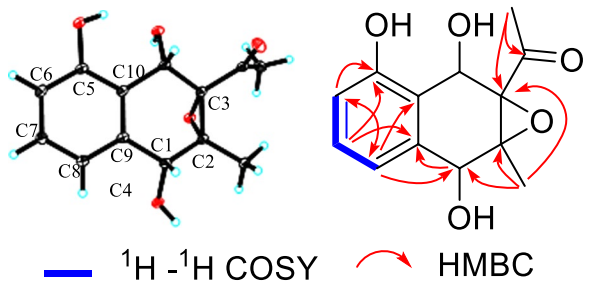

Fig. 5 ^{1}H–^{1}H COSY, HMBC spectra and X-ray crystallographic structure of **5**

fine crystal from acetone was obtained and the absolute configuration of **5** was determined by single crystal X-ray diffraction (CDCC Number: 2158643) (Fig. 5). The result confirmed the planar structure of **5**, and revealed unambiguously the absolute configuration as 1*R*, 2*R*, 3*S*, 4*S*.

2.2 Anti-fungal and anti-inflammatory inhibitory activity

Compounds **1** and **6**–**14** were evaluated for their inhibitory effects against three skin fungi (*Epidermophyton floccosum*, *Trichophyton rubrum*, *Microsporum gypseum*) at a concentration of 100 μM (Table S1), as previously described [28], with terbinafine as positive control. Most of them displayed only weak antifungal activity against the three skin fungi, while compound **9** showed obvious antifungal activities against *E. floccosum* and *M. gypseum* with MIC_{50} values of 2.467 ± 0.03 μM and 4.673 ± 0.077 μM, respectively. In case of the antifungal effects against *E. floccosum* and *M. gypseum,* simple emodin type anthraquinone **9** showed the strongest inhibition, followed by oxyglucoside anthraquinone (**12**) or *C*-glucoside oxanthrones (**13**, **14**), and finally glycosylated seco analogues (**1**, **6**–**8**). These compounds (**1**, **6**–**14**) were also evaluated for their anti-inflammatory activity by using LPS to induce the production of iNOS from mouse monocyte macrophage RAW264.7, with L-NMMA as a positive control. The inhibition rate was shown in Table S2, all 10 anthraquinones showed NO inhibitory activity at a concentration of 50 μM, and the order of their inhibition rates is as follows: **9** > **11** > **12** > **13** > **14** > **8** > **10** > **1** > **6** > **7**. Compound **9** had the strongest anti-inflammatory effect, followed by oxyglucoside anthraquinone, *C*-glucoside oxanthrones and finally seco-anthraquinone glucosides. It is noted that the anti-inflammatory and anti-fungal potential of emodin (**9**) decreased when it become glycosides or seco-anthraquinone cleavaged between C-10 and C-4a.

3 Experimental

3.1 General experimental procedures

UV spectra were given on a UV-2410PC Shimadzu spectrometer. One and two-dimensional NMR spectra were determined on acetone-d_6 and methanol-d_4 with Bruker Ascend-600 and AV-800 spectrometers. Chemical shifts

(δ) were recorded in (parts per million, ppm) scale with TMS (Bruker, Zurich, Switzerland) as an internal standard. Coupling constants were expressed in hertz (Hz). ESI mass spectra were measured on a VG Auto Spec300 spectrometer. High-resolution electro-spray ionization mass (HRESIMS) spectra were performed on an API QSTAR Pular-1 spectrometer. Semi-preparative HPLC was performed on a Hanbon Sci & Tech with Capcell Pak Phenyl (250 mm × 10 mm, 5 μm) and Thermo Hypeersil GOLD aQ (250 mm × 9.4 mm × 5 μm) columns. Analytical HPLC was performed on a Waters 2695 Series HPLC system equipped with a reverse-phase ZORBAX SB-C-18 column (4.6 mm × 150 mm, 5 μm, Agilent Corporation, USA). Column chromatography (CC) was carried out using Sephadex LH-20 (25–100 μm, Pharmacia Fine Chemical Co., Ltd., Uppsala, Sweden), 75–100 μm MCI-gel CHP20P (Mitsubishi Chemical Co. Ltd., Tokyo, Japan), silica gel (100–200 mesh, Qingdao Marine Chemical, Inc., Qingdao, China) and macro-porous absorption resin (D101, Donghong Chemical Co., Ltd., People's Republic of China). Acetonitrile (chromatographic grade) were purchased from XinLanJing (Pennsylvania, USA). Mouse mononuclear macrophage RAW264.7 was purchased from the Shanghai Cell Bank of the Chinese Academy of Sciences, DMEM medium and fetal bovine serum were purchased from BI Company. Griess Reagent, LPS, Terbinafine hydrochloride, DMSO and control drug L-NMMA were purchased from Sigma. *Epidermophyton floccosum*, *Trichophyton rubrum* and *Microsporum gypseum* were purchased from the Medical Fungal Conservation Centre, Chinese Academy of Medical Sciences.

3.2 Plant materials

The roots of *R. crispus* were collected from Yimen town, Xianyang City, Shaanxi Province, in August 2020, and identified by Dr. En-De Liu from Kunming Institute of Botany (KIB), Chinese Academy of Sciences (CAS). A voucher specimen (KIBZL-20200803) is deposited at State Key Laboratory of Phytochemistry and Plant Resource in West China of KIB–CAS.

3.3 Extraction and isolation

The air-dried roots of *R. crispus* (10.0 kg) were crushed into small pieces and extracted with 90% aqueous MeOH at 60 °C (15 L × 4, each time 2 h). The organic solvent was removed under reduced pressure to yield a residue (1.6 kg), which was further extracted with ethyl acetate. After concentrated, the aqueous layer (480 g) was applied to a Sephadex LH-20 column chromatography (CC), eluting with water–methanol (1:0–0:1) to give two fractions (I–II). Fr. I (70 g) was subjected to CC over macroporous resin D101, eluting with H_2O firstly to remove the sugars, and then with 100% MeOH. The yielded MeOH fraction (50.5 g) was subjected to CC over silica gel, eluting with a $CHCl_3$/MeOH gradient system (1:0, 9:1, 8:2, 7:3, 6:4, 1:1, 0:1) to yield 6 fractions, A-F. Fr. A (10 g) was chromatographed on silica gel column with a petroleum ether/ethyl acetate gradient system (1:0, 9:1, 8:2, 7:3, 6:4, 1:1, 0:1) to yield **11** (4.8 mg), **10** (5.0 mg), **9** (100.0 mg). Fr. B (19.5 g) was appplied to RP-18 CC with a MeOH/H_2O gradient system (from 0:1 to 1:0) to afford fractions B1-B4. Fr. B2 (500 mg) was purified by semipreparative HPLC (3 mL/min) with 7% MeCN/H_2O (7:93) containing 0.1% trifluoroacetate to yield **1** (7.0 mg, retention time = 9 min), **6** (12.5 mg, retention time = 7 min), **7** (37.0 mg, retention time = 8 min), **8** (14.0 mg, retention time = 12 min), **12** (1.50 mg, retention time = 14 min), **13** (3.70 mg), **14** (17.0 mg). Fr. C (2.5 g) was separated by chromatography on a Chromatorex ODS column (2.5 cm i.d. × 35 cm) with 10 − 60% MeOH (5% stepwise, each 500 mL) to give Fr. C1 (50 mg) and Fr. C2 (1.0 g). Further, Fr. C1 was separated by semipreparative HPLC (Capcell Pak Phenyl, 250 mm × 10 mm × 5 μm, CH_3CN/H_2O 22:78) to obtain **2** (5.0 mg, retention time = 13.5 min) and **3** (12.0 mg, retention time = 17.3 min), and Fr. C2 was separated by semipreparative HPLC (Thermo Hypeersil GOLD aQ, 250 mm × 9.4 mm × 5 μm, CH_3CN/H_2O 28:72) to obtain **4** (50.0 mg, retention time = 8.0 min), **5** (305.0 mg, retention time = 10.0 min), respectively.

3.3.1 Crispuside A (1)

Yellowish amorphous powder; UV (MeOH) λ_{max} (log ε) 206 (4.4), 274 (3.7) nm. ^{1}H (600 MHz) and ^{13}C (150 MHz) NMR (in methanol-d_4) data, see Table 1. ESIMS *m/z* 449 $[M-H]^-$; HRESIMS *m/z* 449.1094 $[M-H]^-$, (calcd $C_{21}H_{21}O_{11}$: 449.1089).

3.3.2 Naphthalenone A (2)

White amorphous powder, $[\alpha]_D^{19.5}$ + 15.03 (*c* 0.07, MeOH); UV (MeOH) λ_{max} (log ε) 222 (3.1) 270 (2.8), 330 (2.3) nm. ^{1}H (600 MHz) and ^{13}C (150 MHz) NMR (in methanol-d_4) data, see Table 2. ESIMS *m/z* 235 $[M-H]^-$; HRESIMS *m/z* 235.0979 $[M-H]^-$, (calcd $C_{13}H_{15}O_4$, 235.0976).

3.3.3 Naphthalenone B (3)

White amorphous powder; $[\alpha]_D^{19.5}$ + 1.58 (*c* 0.16, MeOH); UV (MeOH) λ_{max} (log ε) 222 (3.1), 270 (2.8), 330 (2.3) nm. ^{1}H (600 MHz) and ^{13}C (150 MHz) NMR (in methanol-d_4) data, see Table 2. ESIMS *m/z* 235 $[M-H]^-$; HRESIMS *m/z* 235.0979 $[M-H]^-$, (calcd $C_{13}H_{15}O_4$, 235.0976).

3.3.4 Naphthalenone C (4)

Yellow amorphous powder; $[\alpha]_D^{25.9}$ + 13.43 (*c* 0.76, MeOH); UV (MeOH) λ_{max} (log ε) 240 (3.1), 330 (2.6) nm. ^{1}H (600 MHz) and ^{13}C (150 MHz) NMR (in methanol-d_4) data, see Table 2. ESIMS *m/z* 233 $[M-H]^-$; HRESIMS *m/z* 233.0814 $[M-H]^-$, (calcd $C_{13}H_{13}O_4$ 233.0814).

3.3.5 (1R,2R,3S,4S)-3-Acetyl-2-methyl-1,4,5-trihydroxy-2,3-epoxynaphthoquinol (5)

White amorphous powder; ^{1}H (500 MHz) and ^{13}C (125 MHz) NMR (in methanol-d_4) data, see Table 2. ESIMS *m/z* 249 $[M-H]^-$.

3.3.6 Single-crystal X-ray diffraction data of 5

Colorless crystal of **5**: $C_{13}H_{14}O_5$, $M=250.24$, $a=7.7634$ (3) Å, $b=8.2971$ (3) Å, $c=9.2218(3)$ Å, $\alpha=90°$, $\beta=107.7570$ (10)°, $\gamma=90°$, $V=565.71$ (4) Å^3, $T=100$ (2) K, space group *P*1211, $Z=2$, μ(Cu Kα) = 0.954 mm^{-1}, 10,180 reflections measured, 2156 independent reflections ($R_{int}=0.0500$). The final R_1 values were 0.0319 [$I>2\sigma(I)$]. The final $wR(F^2)$ values were 0.0821 [$I>2\sigma(I)$]. The final R_1 values were 0.0333 (all data). The final $wR(F^2)$ values were 0.0832 (all data). The goodness of fit on F^2 was 1.064. Flack parameter = 0.17(10). Crystallographic data for the structure of **5** have been deposited in the Cambridge Crystallographic Data Centre (deposition number CCDC, 2,158,643). Copies of the data can be obtained free of charge from the CCDC via www.ccdc.cam.ac.uk.

3.4 The biological assay

The isolates **1** and **6**–**14** were evaluated for their anti-fungal against three skin fungi (*Epidermophyton floccosum*, *Trichophyton rubrum*, *Microsporum gypseum*) and anti-inflammatory activity. For anti-fungal activity, Terbinafine hydrochloride was used as positive control. Fungal broth (5×105 CFU mL^{-1}) and test samples (100 μM) were incubated in 96-well plates at 25 °C for 5 days, A microplate reader was recorded by the absorbance at 625 nm. The experiment also set up the culture medium blank control, fungi control and terbinafine hydrochloride positive drug control.

The anti-inflammatory activity of **1** and **6**–**14** was screened as previously reported method [29]. The mouse mononuclear macrophage RAW264.7 was inoculated to 96 orifice plates and induced by 1.0 μg/mL LPS. At the same time, compounds **1** and **6**–**14** (final concentration 50 μM) was added, and no drug group and L-NMMA positive drug group were taken as controls. After the cells were cultured overnight, the medium was used to detect NO production and the absorbance was measured at 570 nm. MTS was added to the remaining medium to detect the cell survival rate and exclude the toxic effects of the compounds. The formula to calculate the inhibition rate is as follows: NO production inhibition rate (%) = (non-drug treatment group $OD_{570\ nm}$ − sample group $OD_{570\ nm}$)/non-drug treatment group $OD_{570\ nm}\times100\%$.

4 Conclusion

Four new (**1**–**4**) and ten known (**5**–**14**) quinone derivatives were isolated and identified from the roots of *Rumex crispus* L. Compound **1** is a seco-anthraquinone glucoside, while **2**–**4** belong to naphthalenones containing 3,4-dihydronaphthalen-1(2*H*)-one moiety. The absolute configuration of **5** was determined for the first time by X-ray single crystal diffraction. The anti-fungal and anti-inflammatory activity of anthraquinones (**1**, **6**–**14**) was tested, of which compound **9** showed obvious anti-fungal activity. The results indicated that simple emodin type anthraquinone is more potential against skin fungi than its oxyglucosyl, *C*-glucosyl and glycosylated seco analogues.

Supplementary Information

The online version contains supplementary material available at https://doi.org/10.1007/s13659-022-00350-3.

Additional file 1. Supporting information.

Acknowledgements

The authors are grateful to the staffs of the analytical and bioactivity screening groups at the State Key Laboratory of Phytochemistry and Plant Resources in West China, Kunming Institute of Botany, Chinese Academy of Sciences, for measuring the spectroscopic data, anti-fungal, and anti-inflammatory activities.

Author contributions

YXL carried out the experiments and drafted the manuscript; NL and JJL revised the manuscript; DW, HTZand MZ completed samples collection; YJZ designed the experiments, revised the manuscript. All authorsread and approved the final manuscript.

Funding

This research was supported by Ministry of Science and Technology of the People's Republic of China, 2021YFE0103600.

Declarations

Competing interests

The authors declare no competing financial interest.

Author details

[1]State Key Laboratory of Phytochemistry and Plant Resources in West China, Kunming Institute of Botany, Chinese Academy of Sciences, Kunming 650204, People's Republic of China. [2]University of Chinese Academy of Sciences, Beijing 100049, People's Republic of China. [3]Yunnan Key Laboratory of Natural Medicinal Chemistry, Kunming Institute of Botany, Chinese Academy of Sciences, Kunming 650201, People's Republic of China.

Received: 5 May 2022 Accepted: 7 June 2022
Published online: 03 August 2022

References

1. Augustin N, Nuthakki VK, Abdullaha M, Hassan QP, Gandhi SG, Bharate SB. Discovery of helminthosporin, an anthraquinone isolated from *Rumex abyssinicus* Jacq as a dual cholinesterase inhibitor. ACS Omega. 2020;5:1616–24.
2. Demirezer Ö, Kuruüzüm A, Bergere I, Schiewe HJ, Zeeck A. Five naphthalene glycosides from the roots of *Rumex patientia*. Phytochemistry. 2001;56:399–402.
3. Orsolya OG, Ildikó L, Judit H, Gusztáv J, Andrea V. Xanthine oxidase inhibitory activity of extracts prepared from Polygonaceae species. Phytother Res. 2015;29:459–65.
4. Bicker J, Petereit F, Hensel A. Proanthocyanidins and a phloroglucinol derivative from *Rumex acetosa* L. Fitoterapia. 2009;80:483–95.
5. Zhang H, Guo Z, Wu N, Xu WM, Han L, Li N, Han YX. Two novel naphthalene glucosides and an anthraquinone isolated from *Rumex dentatus* and their antiproliferation activities in four cell lines. Molecules. 2012;17:843–50.
6. Vasas A, Orbán-Gyapai O, Hohmann J. The genus *Rumex*: review of traditional uses, phytochemistry and pharmacology. J Ethnopharmacol. 2015;175:198–228.
7. Jeong KS. Extraction characteristics of soluble solid from *Rumex crispus*(curled dock) roots. J Environ Sci Int. 2011;20:1265–72.
8. Zhang Y, Xu H, Chen H, Wang F, Huai H. Diversity of wetland plants used traditionally in china: a literature review. J Ethnobiol Ethnomed. 2014;10:72.
9. Shim KS, Lee B, Ma JY. Water extract of *Rumex crispus* prevents bone loss by inhibiting osteoclastogenesis and inducing osteoblast mineralization. BMC Complementary Med Ther. 2017;17:483.
10. Shariati MA. Bioactive compounds and health benefits of edible *Rumex* species-a review. Cell Mol Biol. 2018;64:27–34.
11. Park ES, Song GH, Kim SH, Lee SM, Kim YG, Lim YL, Kang SA, Park KY. *Rumex crispus* and *Cordyceps militaris* mixture ameliorates production of pro-inflammatory cytokines induced by lipopolysaccharide in C57bl/6 mice splenocytes. Prev Nutr Food Sci. 2018;23:374.
12. Eom T, Kim E, Kim JS. In vitro antioxidant, antiinflammation, and anticancer activities and anthraquinone content from *Rumex crispus* root extract and fractions. Antioxidants. 2020;9:726.
13. Feduraev P, Chupakhina G, Maslennikov P. Variation in phenolic compounds content and antioxidant activity of different plant organs from *Rumex crispus* L. and *Rumex obtusifolius* L. at different growth stages. Antioxidants. 2019;8:237.
14. Minh TN, Van TM, Andriana Y, Vinh LT, Hau DV, Duyen DH, Guzman-Gelani C. Antioxidant, xanthine oxidase, *α*-amylase and *α*-glucosidase inhibitory activities of bioactive compounds from *Rumex crispus* L. Root Molecules. 2019;24:3899.
15. Jiang L, Zhang S, Xuan L. Oxanthrone *C*-glycosides and epoxynaphthoquinol from the roots of *Rumex japonicus*. Phytochemistry. 2007;68:2444–9.
16. Mei R, Liang H, Wang J, Zeng L, Lu Q, Cheng YX. New seco-anthraquinone glucosides from *Rumex nepalensis*. Planta Med. 2009;75:1162–4.
17. Zhang X, Liu F, Feng ZM, Yang YN, Jiang JS, Zhang PC. Bioactive phenylpropanoid esters of sucrose and anthraquinones from *polygonum cuspidatum*. Fitoterapia. 2020;146: 104673.
18. Yang L, Li T, Yang L, Dong L, Chen J. Two-dimensional correlation spectroscopy indicates the infrared spectral markers of the optimum scorching degree of rhubarb (Rhei Radix et Rhizoma) to enhance the anti-inflammatory activity. Spectrochim Acta Part A. 2022;270:120853.
19. Kim G, Xu YJ, Farha AK, Sui ZQ, Corke H. Bactericidal and antibiofilm properties of *Rumex japonicus* Houtt. on multidrug-resistant *Staphylococcus aureus* isolated from milk. J Dairy Sci. 2022;105:2011–24.
20. Liu X, Ma S, Huang Y, Li L. Identification of metabolites of Dachengqi Decoction in human intestinal microflora in vitro by HPLC-QTOF-MS/MS. Tradit Chin Drug Res Clin Pharmacol. 2021;32:1004–11.
21. Yu M, Chen TT, Zhang T, Jia HM, Li JJ, Zhang HW, Zou ZM. Anti-inflammatory constituents in the root and rhizome of *Polygonum cuspidatum* by UPLC-PDA-QTOF/MS and lipopolysaccharide-activated RAW264.7 macrophages. J Pharm Biomed Anal. 2021;195:113839.
22. Wang ZY, Zhao HP, Zuo YM, Wang ZQ, Tang XM. Two new *C*-glucoside oxanthrones from *Rumex gmelini*. Chin Chem Lett. 2009;20:839–41.
23. Yang Y, Yan YM, Wei W, Luo J, Zhang LS, Zhou XJ, Wang PC, Yang YX, Cheng YX. Anthraquinone derivatives from *Rumex* plants and endophytic *Aspergillus fumigatus* and their effects on diabetic nephropathy. Bioorg Med Chem Lett. 2013;23:3905–9.
24. Liu HJ, Chen SH, Liu WY, Liu YY, Huang XS, She ZG. Polyketides with immunosuppressive activities from Mangrove endophytic fungus *Penicillium* sp. ZJ-SY2. Mar Drugs. 2016;14:217.
25. Qi FF, Zhang W, Xue YY, Geng C, Huang XN, Sun J, Lu XF. Bienzyme-catalytic and dioxygenation-mediated anthraquinone ring opening. J Am Chem Soc. 2021;143:16326–21633.
26. Tran TD, Wilson BAP, Henrich CJ, Staudt LM, Krumpe LRH, Smith EA, King J, Wendt KL, Stchigel AM, Miller AN, Cichewicz RH, O'Keefe BR, Gustafson KR. Secondary metabolites from the fungus *Dictyosporium* sp. and their MALT1 inhibitory activities. J Nat Prod. 2019;82:154–62.
27. Nhung LTH, Linh NTT, Cham BT, Thuy TT, Tam NT, Thien DD, Huong PTM, Tan VM, Tai BH, Anh NTH. New phenolics from *Dianella ensifolia* Nat. Prod Res. 2019;35:3063–70.
28. Qu GX, Qi XL, Liu HW, Cai QF. Preliminary screening of traditional Chinese anti-fungi medicines. J Shenyang Pharm Univ. 2002;03:218–20.
29. Xin Y, Xu J, Lv JJ, Zhu HT, Wang D, Yang CR, Zhang YJ. New ent-Kaurane and cleistanthane diterpenoids with potential cytotoxicity from *Phyllanthus acidus* (L.) Skeels. Fitoterapia. 2020;157:105133.

Publisher's Note